

SEISMIC WIDTHS OF ACTIVE CRUSTAL FAULT ZONES

Thomas C. Hanks

U.S. Geological Survey
Menlo Park, California 94025

INTRODUCTION

By way of introducing myself and my subject to a number of people that I have not previously met, I should probably begin with the problem that I am a geophysicist, to be more precise an earthquake seismologist, at least most of the time. As some of you undoubtedly know, a popular notion among my colleagues is that crustal faults are rectangular or circular planes of infinitesimal thickness in an elastic halfspace, occasionally layered. Every once in a while these faults, happily enough, give rise to earthquakes which keep us all off the streets. This is probably a better arrangement than most denizens of earthquake country realize.

However loathsome this notion of crustal fault zones might be to serious students of them, it nevertheless has some basis in fact. Figure 1 displays the observed ground motion at El Centro, California, of the Borrego Mountain earthquake (Apr. 9, 1968; $M_L = 6.4$) and ground motion computed for this source-station pair on the basis of a model the parameters of which are sketched at the top of the figure. Just to be perverse about this matter, let me also point out that the faulting motion has been simulated by two point sources; the "fault" in this case not only has vanishing width, it also has vanishing in-plane dimension. Mathematically speaking, there is no fault at all, and in view of the remarkable agreement, by seismological standards, between the observed and synthetic ground motion at El Centro, this situation, however nonphysical and irrelevant it may seem, is not to be casually dismissed. Geologically speaking, of course, there is a fault involved, and some 31 km of it broke during the Borrego Mountain earthquake (Clark, 1972).

The conclusion to be drawn here, apparently, is that on time scales of hundreds of seconds or less that are associated with rupture of crustal

fault zones in the course of even the very largest earthquakes, the mechanics of crustal fault zones and of the immediate failure zone of interest can be described largely if not wholly by elastic--more correctly equivalent-elastic--processes. By equivalent-elastic is meant the replacement of the failure region with an interior boundary surface on which elastic displacements or tractions are specified, but in virtually every case this can be reduced to a plane across which exists an elastic displacement discontinuity (if not a point source of double couple moment).

There is considerable justification for and application of this result seismologically, and it is implicit in virtually every earthquake source mechanism analysis based on the radiated field. This same result is, moreover, implicit in the estimation of seismic slip rates via cumulative seismic moment sums (Brune, 1968; Davies and Brune, 1971). For a number of major plate boundaries, the seismic slip rates so obtained with 80 years of seismic data are in remarkable agreement with plate motion rates over millions of years, as obtained from magnetic anomalies in oceanic areas or from geological data in continental ones.

But even if we admit that this seismological notion of faulting and faults is correct for such short time scales--and we might as well to the extent that this notion is at least consistent with the available information--we still may ask: What if anything does it have to do with the development of the substantial anelastic deformation that is commonly associated with throughgoing crustal fault zones across an often significant dimension normal to the plane of offset? The answer can only be--as any defender of the true faith knows--not much.

There is, however, a very wide range in scale between hundreds of seconds and the million of years involved in the development of a through-

going fault or major plate boundary. On what intermediate time scale, then, does the non-planar, volumetric, anelastic deformation along fault zones begin to develop? I will address this issue here with aftershock and regional seismicity data taken over a time scale of weeks to years. Briefly, the result is this: even on a time scale of weeks to years, a number of fault segments reveal distinctly volumetric deformation, if the earthquake locations are as good as they are advertised to be. With these data, however, we cannot sample whatever anelastic deformation may be occurring along the fault zone. Indeed, for all these data can show us, all of the deformation may only be elastic displacement discontinuities on multiple rupture planes, the typical separation of which also involves a wide range of distance scales.

SOME EXAMPLES

1. Central California

Figure 2 displays the seismicity of central California in the year 1977 (unpublished data of J. P. Eaton); in general location errors are several km, although relative locations in specific areas are undoubtedly better. The location error, however, depends on the station distribution local to the area of interest, and the distribution of stations in Figure 2 is far from uniform.

While it is commonly agreed that the San Andreas fault is the boundary between the Pacific and North American plates in this region, it is plain that a significant portion of the seismicity in Figure 2 has no immediate relationship with the San Andreas. Even where the San Andreas fault is clearly lined by seismicity (the northwesterly trending alignment between 36° and 37° N), significant off-fault activity is occurring. North of 37° N (near San Juan Bautista) the San Andreas fault has very little seismic expression at the present time, but a seismically active zone of considerable breadth parallels

the San Andreas fault some 50 km to the east of it. This zone of seismic deformation is traversed by a complex of northwesterly-trending but apparently not continuous faults.

There is, moreover, considerable additional evidence from the many fault plane solutions available for the region of Figure 2 (W. H. K. Lee, unpublished data), geodetic data (Thatcher, 1975), and "instantaneous" plate motion calculations (Minster and Jordan, 1978), not to mention, of course, the longer term geologic data (e.g., Graham and Dickinson, 1978), that deformation in the central California region, at least above 37°N, involves more than simple block motion across the San Andreas fault. Perhaps somewhat surprisingly, these indications are amply, if only qualitatively, portrayed by one year of seismicity data.

2. Imperial Valley

Figures 3a and 3b present 6 years of seismicity data for the Imperial Valley, California (Johnson, 1978). Figure 3a plots all of the events that can be located, while Figure 3b presents only the high-quality locations. The belt of seismicity 5 to 10 km in width that extends from the Imperial fault on the south to the San Andreas fault to the north is related to a fault system comprised, at least in part, of a series of ridge-transform pairs. While this geometry surely leads to some of the apparent diffusion of epicenters, it seems almost impossible to associate all of this seismicity to slip along a single, piecewise continuous set of simple fault planes. The block between the Imperial and Brawley faults near their intersection south of Brawley is being deformed through a significant volume. Similarly, the connection between the San Jacinto fault zone and the Imperial fault, provided that it even exists in some meaningful sense, is plainly complicated, in view of the distribution of epicenters near SUP. Altogether,

the seismic deformation in the Imperial Valley occurs over a significant dimension normal to the trend of right lateral slip in this region, and, again, geodetic data also reveal a pattern of distributed deformation in the Imperial Valley (Savage et al., 1979).

3. Aftershocks of the Parkfield earthquake (June 28, 1966; $M_L = 5.5$)

Figures 4a and 4b display the well-located aftershocks of the Parkfield, California, earthquake in plan and cross-section views, respectively (from Eaton et al., 1970a). This study set international standards for micro-earthquake locations, the essential ingredient being the small station-spacing that is now typical for most of the seismically active regions of California. The location accuracy is about a kilometer, if not somewhat better in the center of the array. Both in plan and cross-section, these aftershocks cluster remarkably close to the San Andreas fault. Indeed, given the location accuracy, these aftershocks define a single, simple plane of failure, over a 30 km length and 12 km down-dip width (the heavy line in Figures 4a and 4b). 98% of the more than 200 aftershock focal mechanisms suggest an equally simple model of failure in the course of the aftershock sequence.

Even so, the slight dogleg of approximately one km offset in the active fault trace in Cholame Valley (near 15 km in the coordinate system of Figure 4a) is reproduced by the aftershock distribution, suggesting control by a deeper seated structure. It is probably not coincidental that there is a strong clustering of aftershocks in this region, that most of the larger aftershocks occurred here as well, and that four of the five anomalous fault plane solutions occurred in this region of offset (Eaton et al., 1970a).

Because this was the first such detailed seismicity study, at least in the United States, and because of the remarkable planar geometry of the

aftershock zone at Parkfield, this study has probably contributed significantly to the idea that faults are simple planes in layered elastic half-spaces. With the exception of the dogleg area, this is indeed the case at Parkfield, as it is for much of the central reach of the San Andreas fault between Parkfield and San Juan Bautista, wherein the fault is relatively straight and continuous and faulting motion is dominated by aseismic slip. This is not always the case in this region, however, as indicated by the distribution of aftershocks of a magnitude 4 earthquake in Bear Valley (Figures 5a and 5b) (Eaton et al., 1970b). Moreover, a recent detailed examination of seismicity patterns in Bear Valley are reminiscent of the Parkfield dogleg, with earthquakes concentrating in just those regions where offset of the active trace of the San Andreas fault occurs (Bakun et al., 1979).

4. Aftershocks of the Borrego Mountain earthquake (Apr. 9, 1968; $M_L = 6.4$)

In striking contrast to the Parkfield earthquake, two months of aftershocks (April 12 to June 12, 1968) of the Borrego Mountain, California, earthquake reveal a very complicated spatial pattern (Figures 6a and 6b; Hamilton, 1972). Location accuracy for epicenters within the closure of the array is approximately one km, degrading to several km just outside the net. Depth resolution is estimated to be 2 km near the zone of surface faulting along the Coyote Creek fault. Significant aftershock activity was stimulated at distances of 15 to 20 km away from the observed surface faulting, on both sides of it.

Quite apart from the seismicity well removed from the surface ground breakage, it seems difficult to associate the remaining seismicity with a single plane of failure, or even a small number of failure planes. Rather, the aftershocks are occurring through a significant dimension normal to the

observed trend of faulting. The multiplicity of aftershock fault plane solution orientations and types (Hamilton, 1972) also indicate considerable complications in the strain release occurring in the course of the aftershock sequence.

5. Aftershocks of the San Fernando earthquake (Feb. 9, 1971; $M_L = 6.4$)

As a final--and the most complicated--example, we consider the aftershocks of the San Fernando, California, earthquake. This earthquake is, by far, the best studied earthquake in the history of our science and is associated with great seismologic and geologic complexity. Even at an early date, it was recognized that there were at least four spatially distinct groups of aftershocks (Hanks et al., 1971; Wesson et al., 1971; Whitcomb, 1971), and these are indicated in Figure 7a. Earthquakes clustering in the hypocentral region (I) have locations and focal mechanisms similar to the mainshock. The lineament of region II, however is consistent with a nearly vertical, left-lateral tear fault in the basement beneath the main thrust plane, that steps the thrust plane down to the west (Figure 7b). The eastern group of aftershocks (III) represents a complicated region of strain release, with depths generally less than the inferred depth to the main thrust plane at the appropriate latitude and with a variety of focal mechanism types. The fourth region, interior to the first three and the zone of surface faulting to the south, is characterized by the general absence of aftershocks. Yet it is just this region wherein the main thrust plane lies. "Plane" is used loosely here, since, at the simplest, a thrust surface with increasing dip to the north is required (Hanks, 1974).

In view of these complications, it will not be surprising that the aftershocks, when projected on a single cross-section normal to strike, reveal a pattern of general chaos. They do (Figure 7c, R. L. Wesson, unpub-

lished data). At any particular horizontal distance, aftershocks typically occupy a range in depth of 7 km or more. Quite apart from the other complications, it is most unlikely that a single, simple surface of thrusting will suffice to explain the thrust faulting aftershocks.

DISCUSSION

There is abundant evidence in seismicity data obtained in the past decade, then, that crustal fault zones at depth are at least as complicated as their surface expressions--and in several cases are considerably more so. Nevertheless, there is certainly a matter of degree involved. In central California between 36 and 37°N, where the San Andreas fault movement is dominated by aseismic slip, the fault is relatively simple, straight and continuous--and the great bulk of the seismicity, as well as the geodetically determined displacements, is also immediately associated with the San Andreas. More geologically complicated regions have more diffuse seismicity and strain accumulation patterns.

Of particular interest is the seismic expression of small-scale (\approx 1 km) features of the active fault trace that persist to considerable depth (5 to 10 km) (Eaton et al., 1970; Bakun et al., 1979). Although the connection between seismicity and active crustal faults has long been recognized, as has the value of detailed studies of each, the mechanical connections between fault zone heterogeneity, seismicity patterns, and the detailed geometry of active fault traces are only just now being sought by the seismological community. Much potential for earthquake mechanism studies and for earthquake hazards analysis in several contexts is yet to be realized.

Perhaps the broadest conclusion to be drawn from the observations summarized here is that crustal faults cannot be simple, highly localized zones of weakness surrounded by otherwise strong upper crustal material. In most

cases, shear stress is accumulating over considerable dimension (tens of kilometers or more) normal to major faults and can be released by seismogenic failure over a comparable dimension, which can only mean that there can be no drastic reduction in material strength associated with the fault itself.

- All C. R., T. C. Hanks, and J. H. Whitcomb, Seismological studies of the San Fernando earthquake and their tectonic implications, Bull. Calif. Div. Mines Geol. 196, 257-262, 1973.
- Bakun, W. H., R. M. Stewart, C. G. Bufe, and S. M. Marks, Implication of seismicity for failure of a portion of the San Andreas fault, Bull. Seismol. Soc. Amer., submitted, 1979.
- Brune, J. N., Seismic moment, seismicity, and rate of slip along major fault zones, J. Geophys. Res. 73, 777-784, 1968.
- Clark, M. M., Surface rupture along the Coyote Creek fault, U.S. Geol. Survey Profess. Paper 787, 55-86, 1972.
- Davies, G. F., and J. N. Brune, Regional and global fault slip rates from seismicity, Nature 229, 101-107, 1971.
- Eaton, J. P., M. E. O'Neill, and J. N. Murdock, Aftershocks of the 1966 Parkfield-Cholame, California, earthquake: a detailed study, Bull. Seismol. Soc. Amer. 60, 1151-1197, 1970a.
- Eaton, J. P., W. H. K. Lee, and L. C. Pakiser, Use of microearthquakes in the study of the mechanics of earthquake generation along the San Andreas fault in central California, Tectonophysics 9, 259-282, 1970b.
- Graham, S. A., and W. R. Dickinson, Evidence for 115 kilometers of right slip on the San Gregorio-Hosgri fault trend, Science 199, 179-181, 1978.
- Hamilton, R. M., Aftershocks of the Borrego Mountain earthquake from April 12 to June 12, 1968, U.S. Geol. Survey Profess. Paper 787, 31-54, 1972.
- Hanks, T. C., The faulting mechanism of the San Fernando earthquake, J. Geophys. Res. 79, 1215-1229, 1974.
- Hanks, T. C., T. H. Jordan, and J. B. Minster, Precise locations of aftershocks of the San Fernando earthquake 2300 (GMT) February 10 - 1700

- February 11, 1971, U.S. Geol. Survey Profess. Paper 73, 23, 1971.
- Heaton, T. H., and D. V. HelMBERGER, A study of the strong ground motion of the Borrego Mountain, California, earthquake, Bull. Seismol. Soc. Amer. 67, 315-330, 1977.
- Johnson, C. E., I. CEDAR - An approach to the computer automation of short-period local seismic networks, II. Seismotectonics of the Imperial Valley of southern California, Ph.D. Thesis, California Institute of Technology, Pasadena, 1979.
- Minster, J. B., and T. H. Jordan, Present-day plate motions, J. Geophys. Res. 83, 5331-5354, 1978.
- Savage, J. C., W. H. Prescott, M. Lisowski, and N. King, Deformation across the Salton Trough, 1973-1977, J. Geophys. Res. 84, in press, 1979.
- Thatcher, W., Strain accumulation on the northern San Andreas fault zone since 1906, J. Geophys. Res. 80, 4873-4880, 1975.
- Wesson, R. L., W. H. K. Lee, and J. F. Gibbs, Aftershocks of the earthquake, U.S. Geol. Survey Profess. Paper 733, 24-29, 1971.
- Whitcomb, J. H., Fault-plane solutions of the February 9, 1971, San Fernando earthquake and some aftershocks, U.S. Geol. Survey Profess. Paper 733, 30-32, 1971.

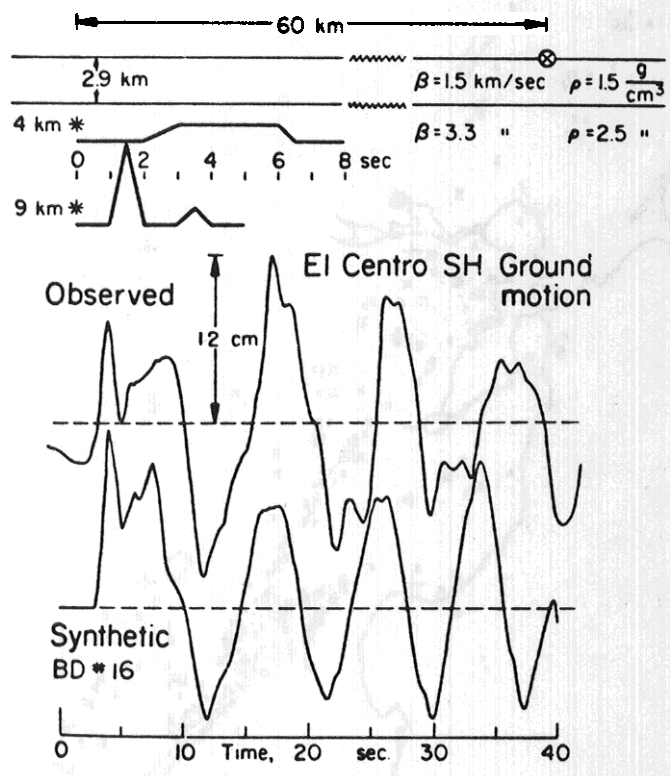
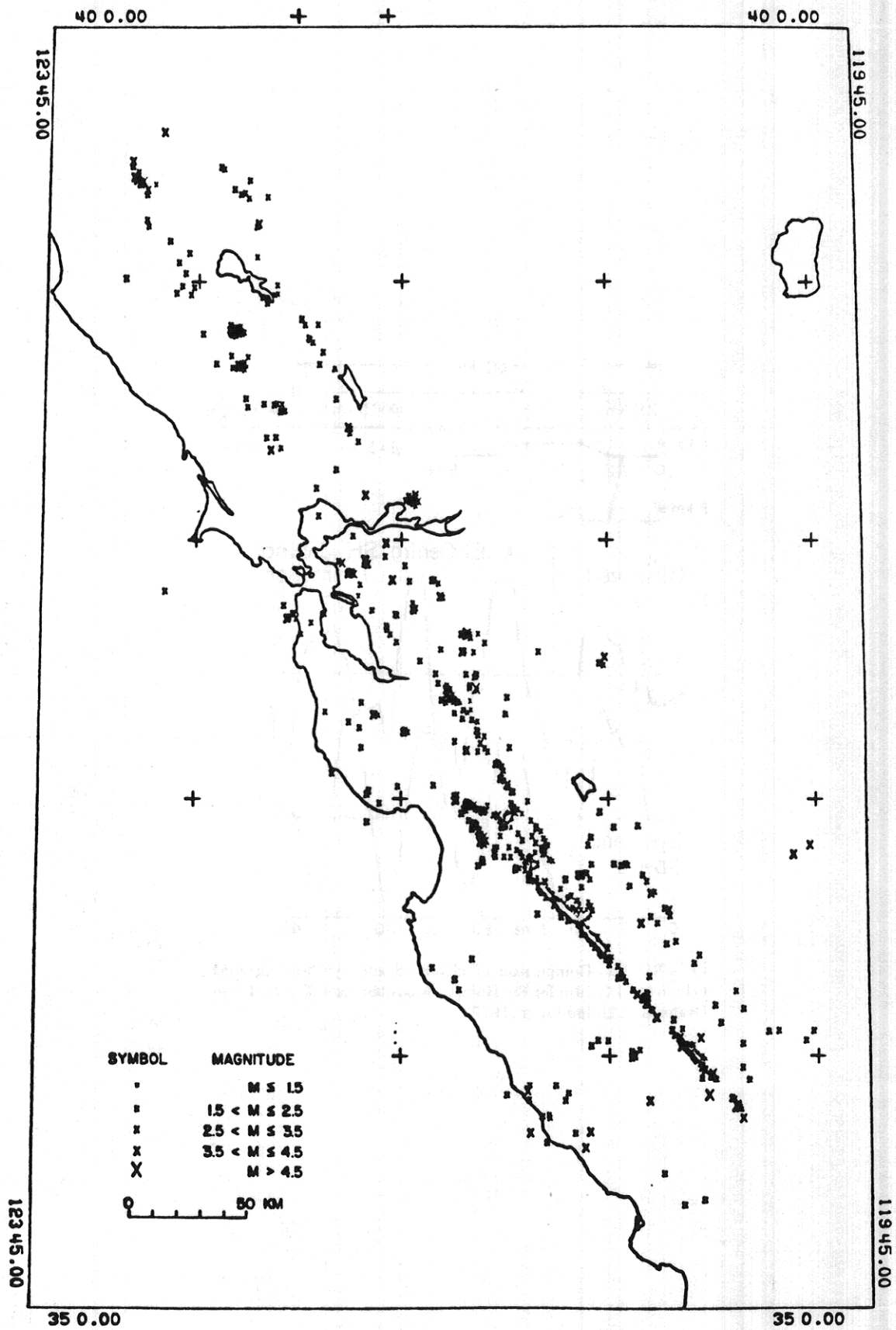


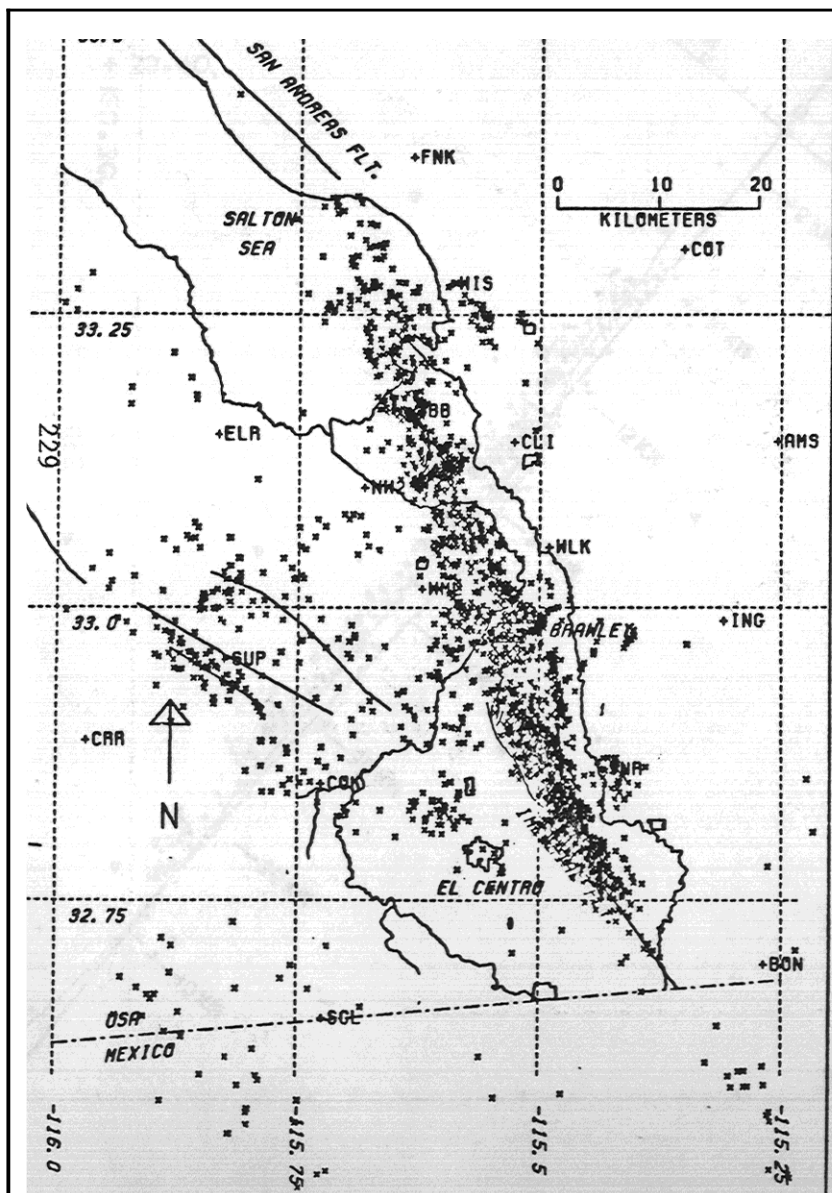
FIGURE 2.5 Comparison of observed and synthetic ground motion at El Centro for the Borrego Mountain earthquake. From Heaton and Helmberger (1977).

1977 EARTHQUAKES - 1:750000 (SCREENED)



(a)

1973 - 1978



(b)

1373 - 1373

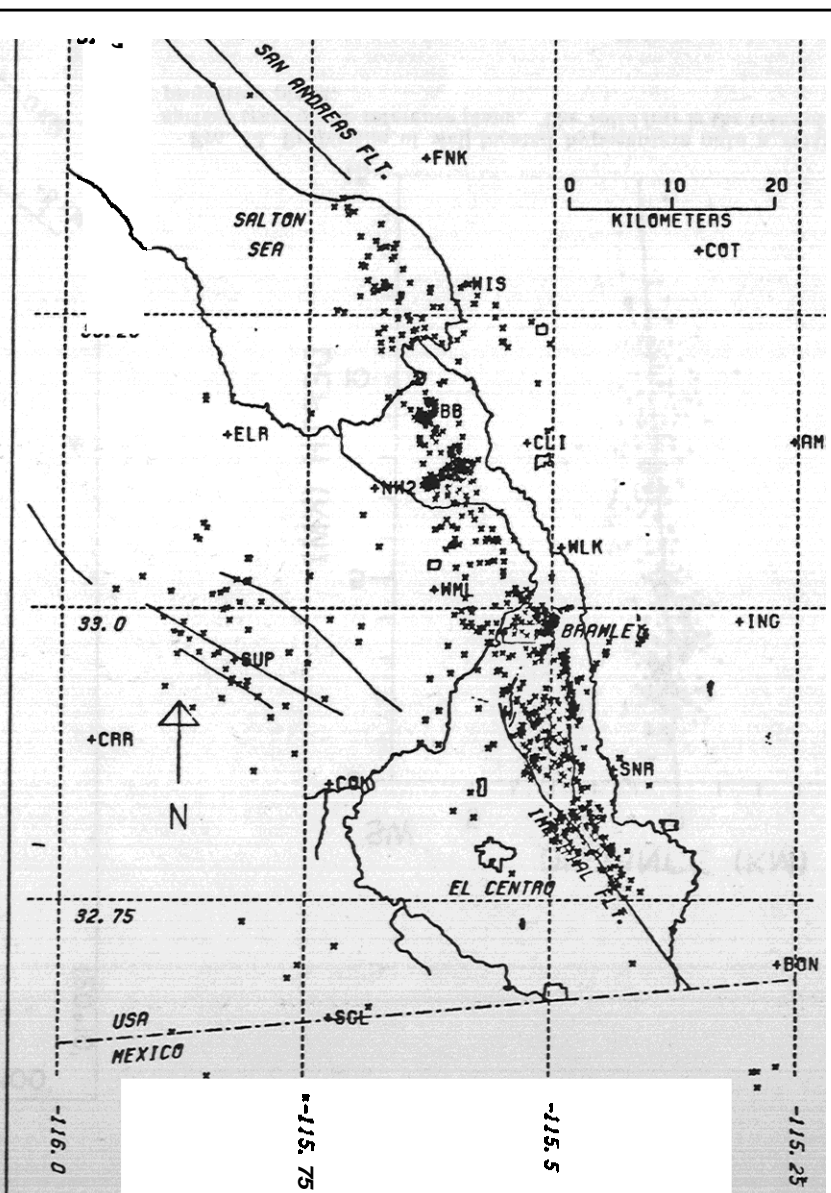


Figure 2

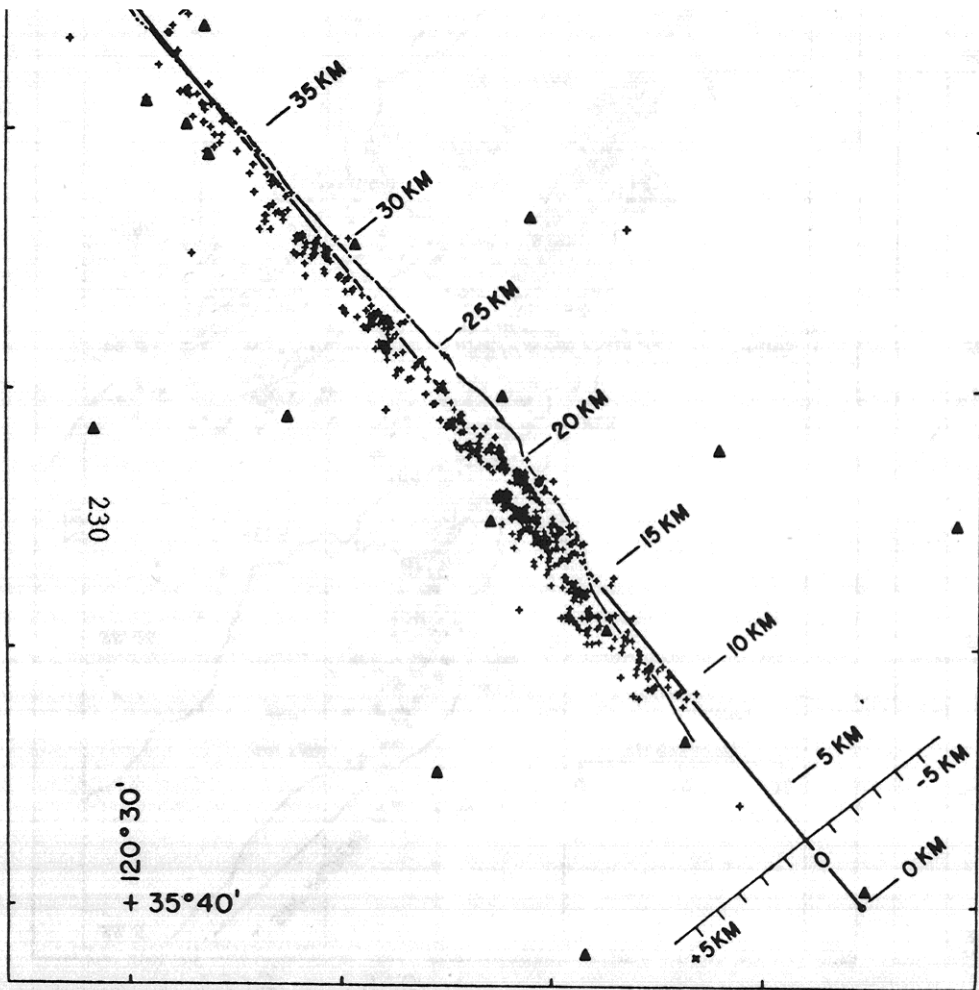


FIG. 9. Epicenters of the well-located aftershocks (July 1 to September 15) and the zone of surface fracturing of the Parkfield-Cholame earthquake. Epicenters are indicated by crosses, seismograph stations by triangles, and the zone of surface fracturing by the heavy solid and dashed curves. The surface outcrop of the reference plane (heavy straight line) is the longitudinal axis of a coordinate system, with origin near station 6, used in the analysis of the distribution of the hypocenters.

(a)

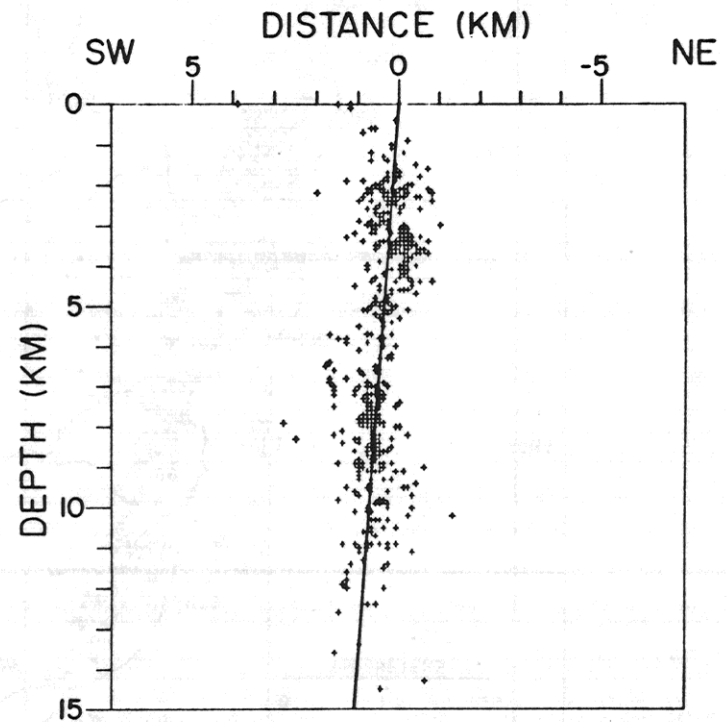


FIG. 10. Projection of well-located hypocenters onto a vertical plane perpendicular to the surface trace of the reference plane. The solid line is the trace of the fitted reference plane on the projection plane.

(b)

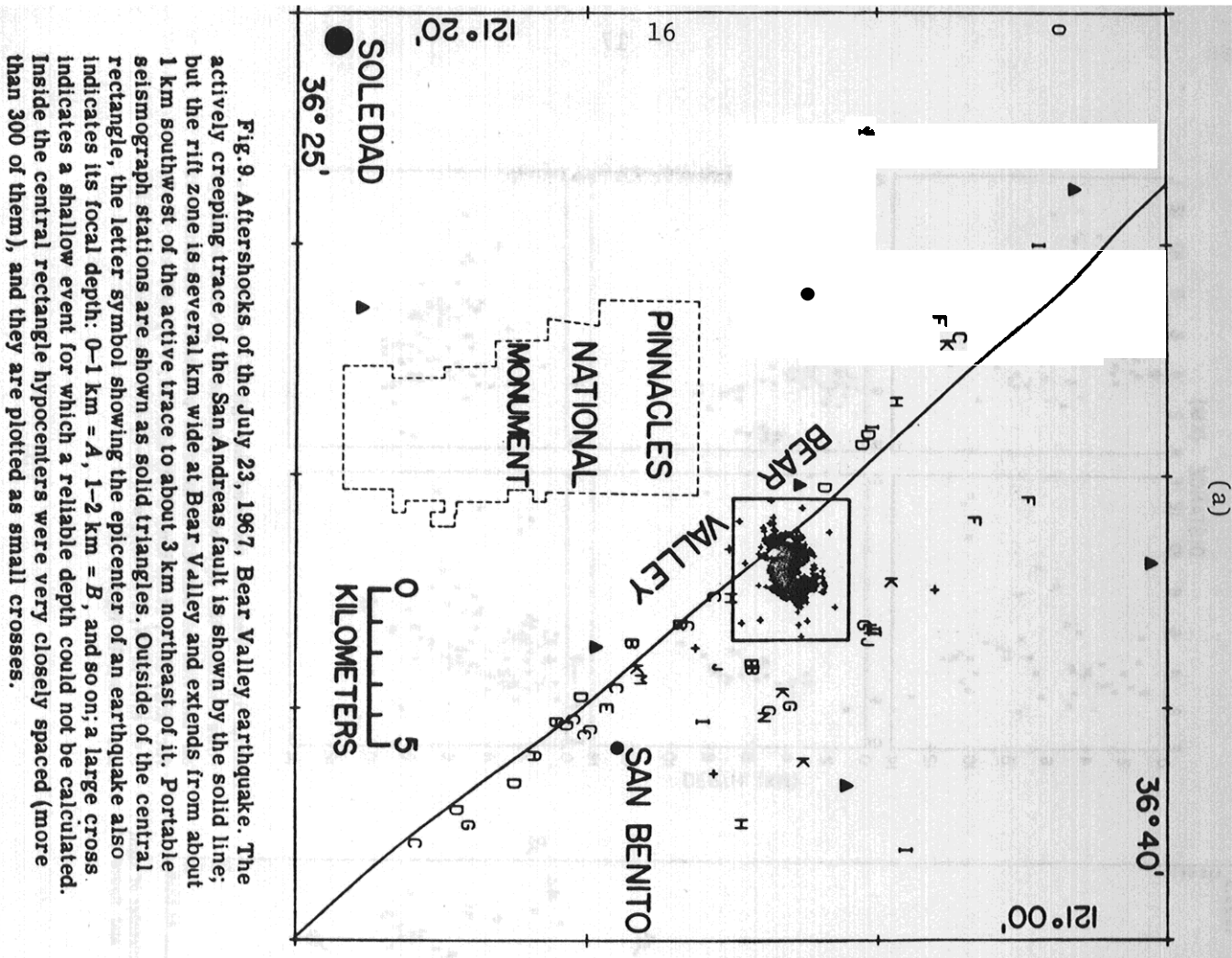


Fig. 9. Aftershocks of the July 23, 1967, Bear Valley earthquake. The actively creeping trace of the San Andreas fault is shown by the solid line; but the rift zone is several km wide at Bear Valley and extends from about 1 km southwest of the active trace to about 3 km northeast of it. Portable seismograph stations are shown as solid triangles. Outside of the central rectangle, the letter symbol showing the epicenter of an earthquake also indicates its focal depth: 0-1 km = A, 1-2 km = B, and so on; a large cross indicates a shallow event for which a reliable depth could not be calculated. Inside the central rectangle hypocenters were very closely spaced (more than 300 of them), and they are plotted as small crosses.

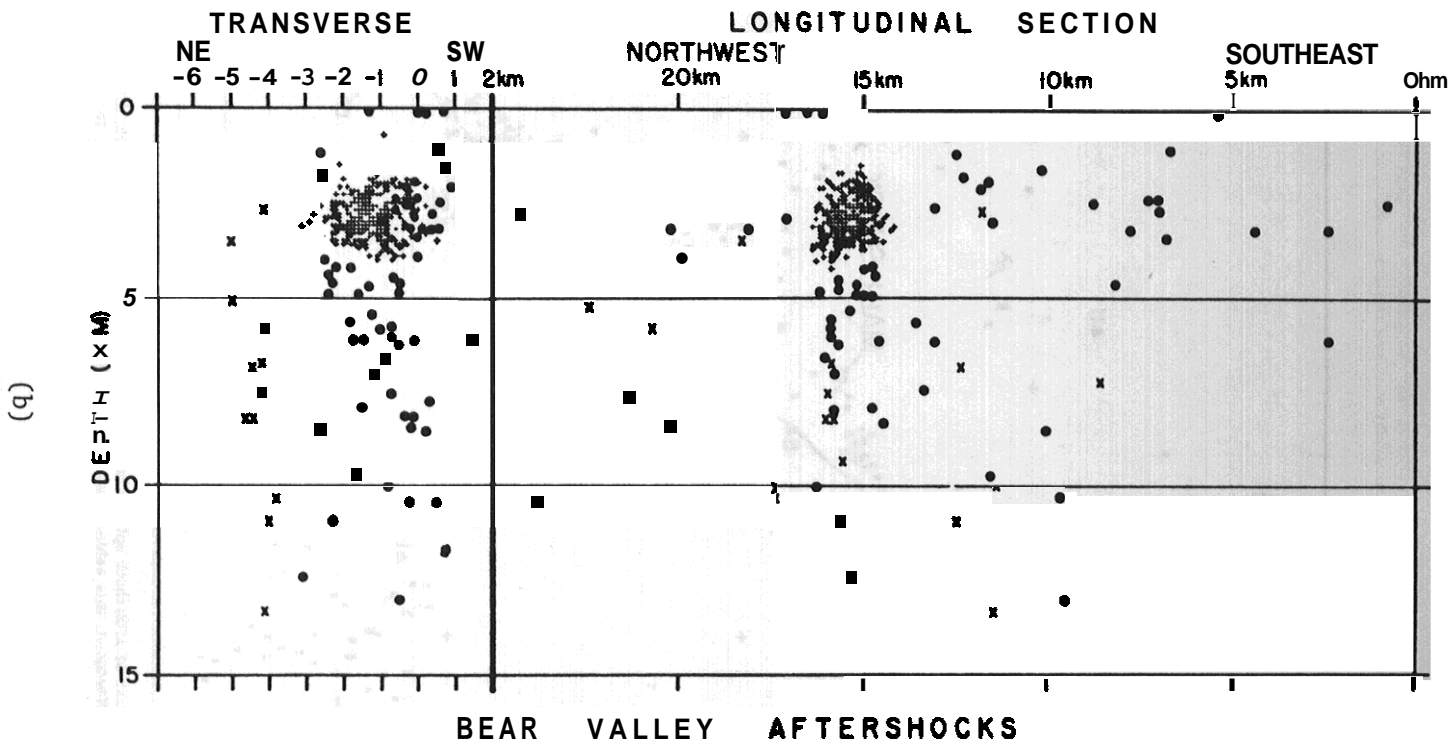


Fig. 10. Bear Valley aftershocks projected onto vertical planes perpendicular (left) and parallel (right) to the actively creeping trace of the San Andreas fault. Aftershocks in the dense cluster of events around the hypocenters of the main shock are plotted as crosses (many were "lost" because of superposition). Aftershocks that lay northeast of the rift zone (more than 3.3 km northeast of the active trace) are plotted as large X's. Other aftershocks are plotted as solid circles.

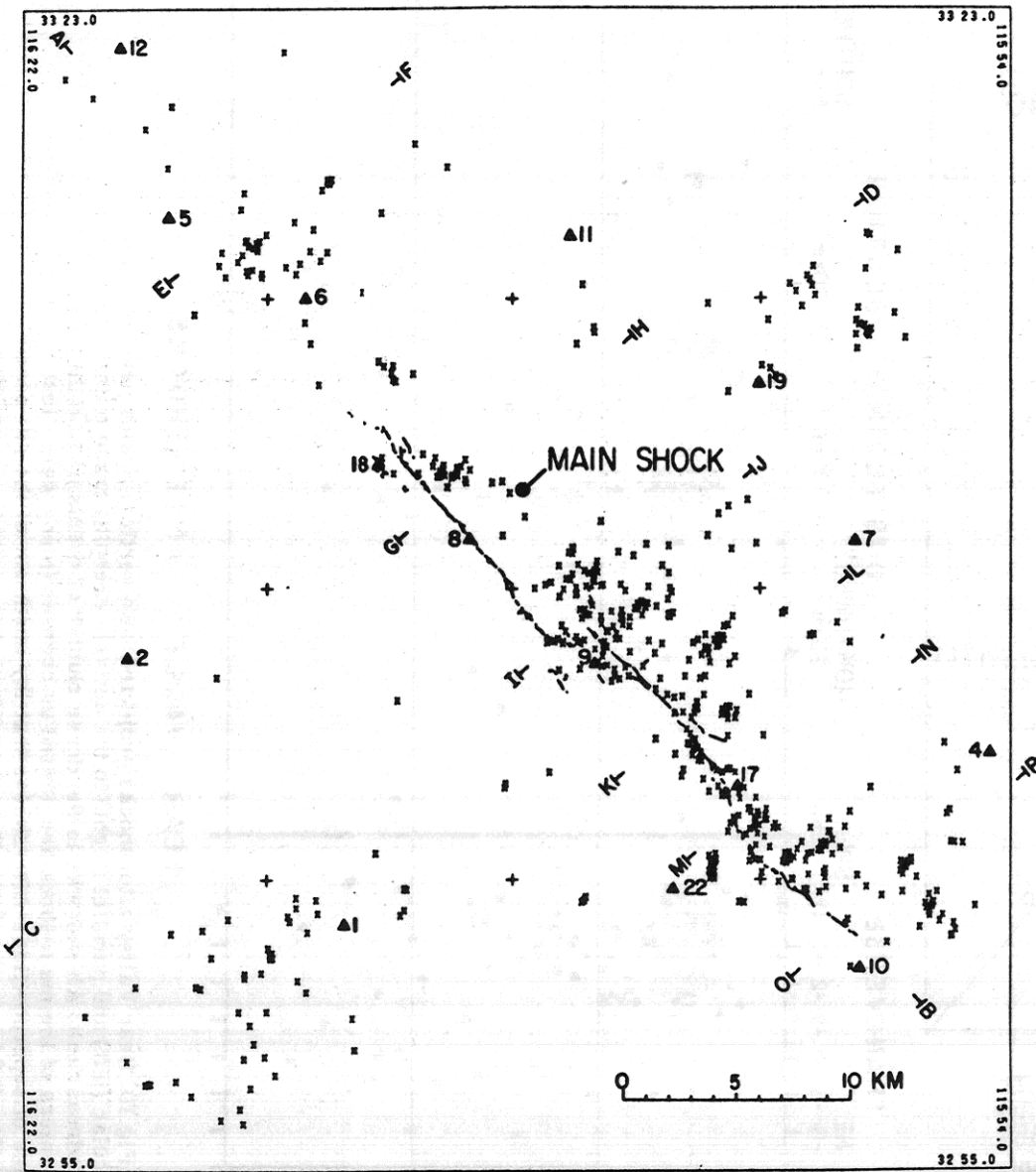


FIGURE 13. — Detailed map of aftershock epicenters (crosses), ground breakage (after Clark, this volume), epicenter of main shock (Allen and Nordquist, this volume), and lines of vertical sections for figure 15 (A-B, C-D) and figure 16 (E-F, etc.)

(a)

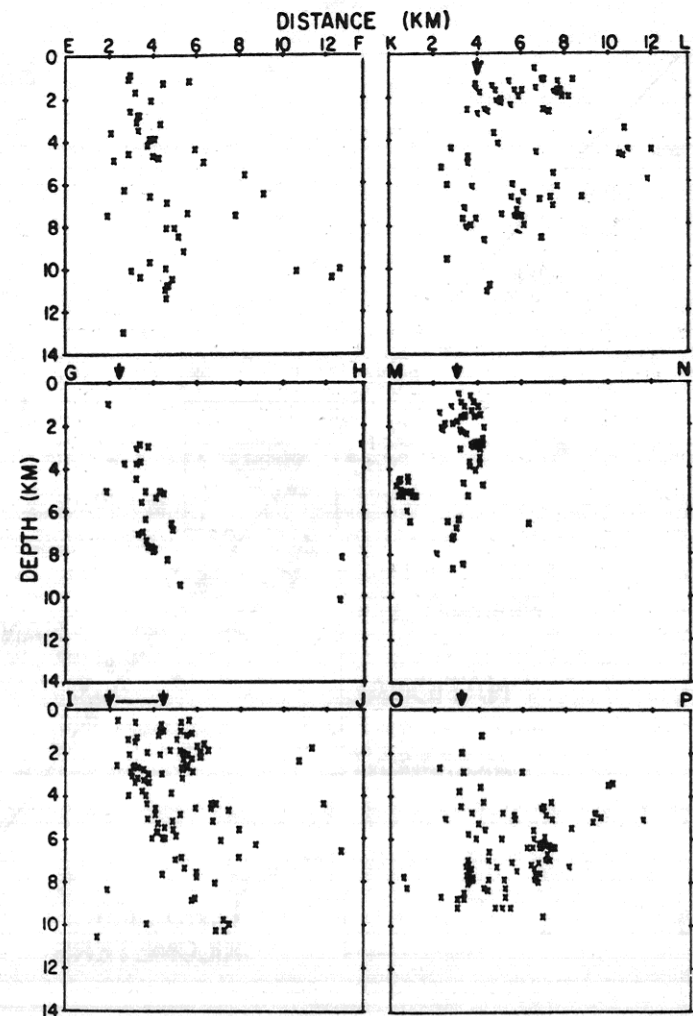
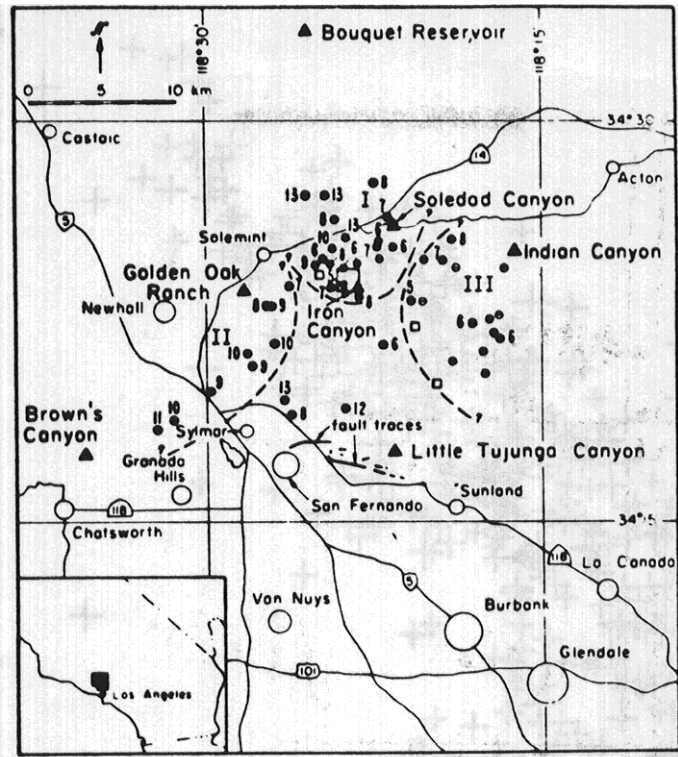


FIGURE 16. — Vertical sections through aftershock zone. Arrows indicate the approximate position of ground breakage on the line of section. Maximum projection distances of foci are: E-F, 11.42 km; G-H, 4.24 km; I-J, 3.92 km; K-L, 2.47 km; M-N, 2.40 km; and O-P, 4.73 km. Lines of section are shown in figure 13.

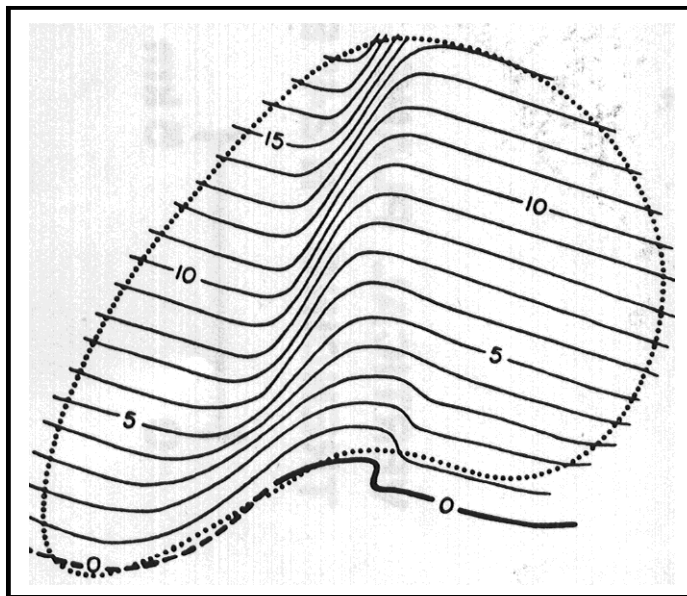
(b)



(a)

Hanks et al (1971)

FIGURE 1.—Distribution of aftershocks of the San Fernando earthquake, in the time interval 2300 (GMT) February 10-1700 February 11, 1971. The larger open square is the main-shock epicenter; the three smaller squares are epicenters for three events $M_L > 4.5$. Solid triangles locate the portable seismograph stations. Numbered solid circles are aftershock locations with the depth (km) as indicated. Open circles with an interior line are shallow aftershocks ($h < 6$ km). Roman numerals denote groupings of aftershocks: I = epical group, II = Chatsworth segment, III = eastern group. fault traces after the section by Kamb and others in this report.



(b)

Allen et al (1973)

Figure 5.—Schematic structural contour map showing simplified contours (in km) a fault plane and showing monoclinial flexure that might explain strike-slip aftershock mechanisms on steep west-dipping flank of flexure in fault surface.

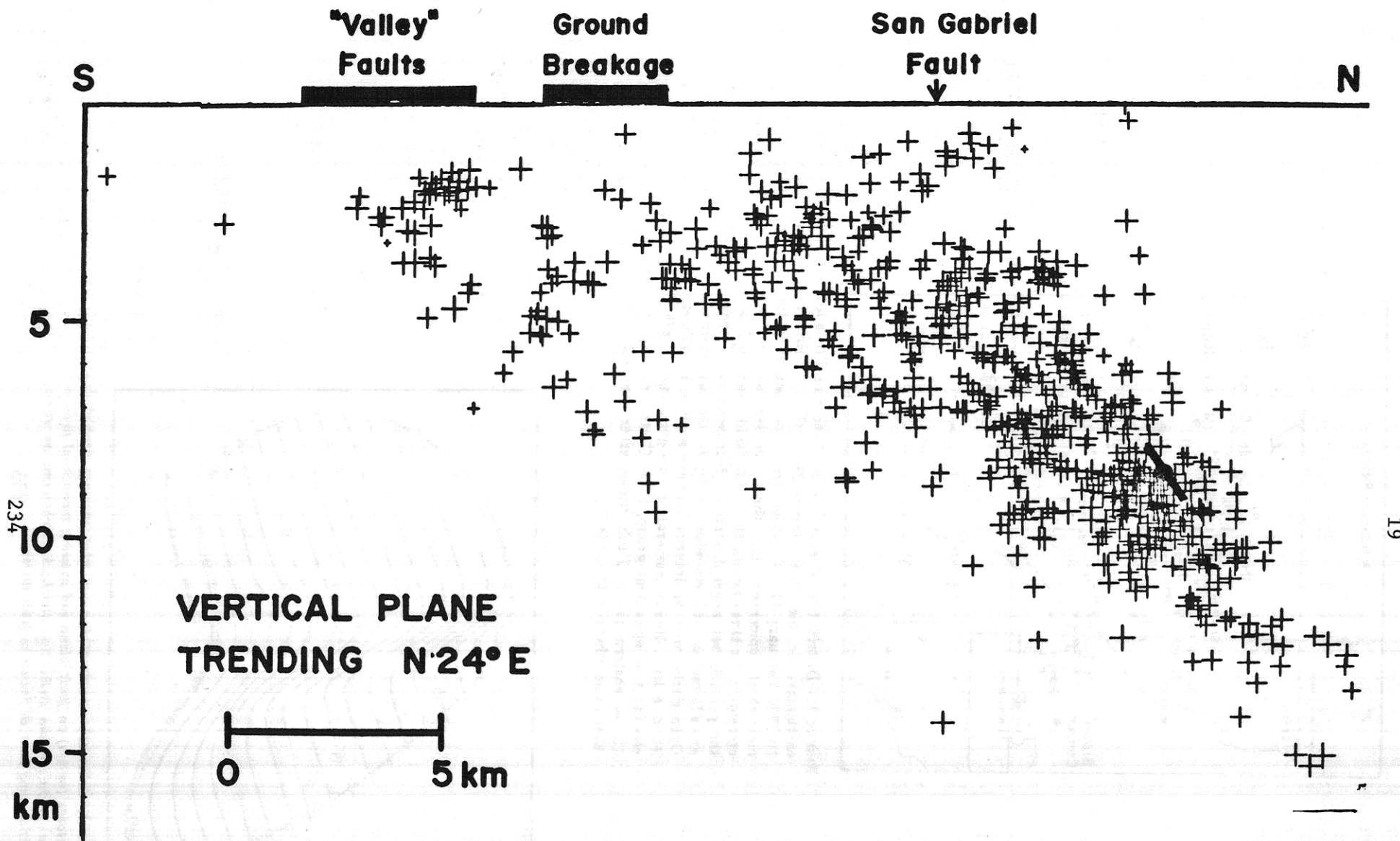


Figure 7c